



Contents lists available at ScienceDirect

Spectrochimica Acta Part A: Molecular and Biomolecular Spectroscopy

journal homepage: www.elsevier.com/locate/saa

Properties of a furan ring-opening reaction in aqueous micellar solutions for selective sensing of mesalazine



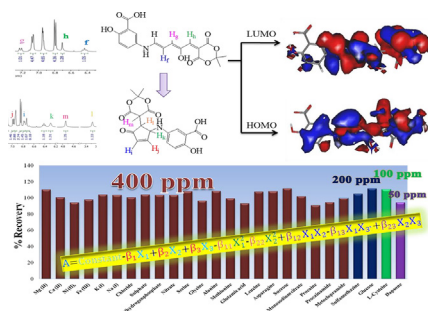
Leila Sabahi-Agabager, Habibollah Eskandari*, Farough Nasiri, Amir Nasser Shamkhali, Somayyeh Baghi Sefidan

Department of Chemistry, Faculty of Basic Sciences, University of Mohaghegh Ardabili, Ardabil 56199-11367, Iran

HIGHLIGHTS

- Mesalazine is determined by spectrophotometry using a furan ring-opening reaction.
- Mesalazine is selectively assayed with a wide linearity range (155-fold).
- CCD study showed that absorbance is dependent to the interactions of the parameters.
- ^1H NMR studies showed that the colored product is being changed to a cyclic isomer.
- Density functional theory shows that the colored product is excited locally.

GRAPHICAL ABSTRACT



ARTICLE INFO

Article history:

Received 24 November 2020
 Received in revised form 26 February 2021
 Accepted 13 April 2021
 Available online 17 April 2021

Keywords:

Mesalazine
 Furan ring-opening reaction
 Donor-acceptor Stenhouse adducts
 Central composite design
 Density functional theory

ABSTRACT

A novel and efficient non-azo formation based method was developed for trace sensing of mesalazine (MES), a pharmaceutical aromatic amine. MES was simply coupled with a Meldrum's activated furan (MAF) reagent via a furan ring opening reaction to form a colored product. The intense purple colored solution was detected at 575 nm. The reaction of MES with MAF was monitored by employing ^1H NMR spectroscopy and mass spectrometry. In addition, density functional theory (DFT) was applied to optimize the structure of the colored product and its λ_{max} (the wavelength of maximum absorbance) in dimethyl sulfoxide and water. The colored product was considered in three possible structures, and the most possible structures in dimethyl sulfoxide and in water were identified by employing the DFT calculations. Both of the most possible structures indicated only a local excitation in their λ_{max} and no charge transfer was observed. However, one of the structures in dimethyl sulfoxide presented charge transfer properties occurring through N=C=C moiety. A univariate optimization method was also used to attain the optimum condition for analysis. In addition, the dependence of the analytical response on the three main affecting parameters (reaction time (X_1), Triton X-100 concentration (X_2) and MAF concentration (X_3)) was identified by employing a central composite design (CCD) approach. The CCD study showed that the analytical response depends complexly on the parameters. Beer's law was obeyed within the range of 0.06–9.30 $\mu\text{g mL}^{-1}$ of MES (155 fold linearity) at 575 nm, under the optimum condition introduced by the CCD approach. Also, the limit of detection was obtained 0.04 $\mu\text{g mL}^{-1}$ of MES. The method showed precision (as relative standard deviation) and accuracy (as recovery) within the ranges of 0.6–3.2 % and 96.3–100.8%, respectively. Various organic and inorganic species, amino-

* Corresponding author.

E-mail address: heskandari@uma.ac.ir (H. Eskandari).

pharmaceuticals, and amino acids were tested to evaluate the selectivity of the method. The selectivity of the analytical method was satisfactory. The method was successfully applied for detection of MES in various water matrices and pharmaceutical tablets.

© 2021 Elsevier B.V. All rights reserved.

1. Introduction

The colored products during the ring opening reactions of furan derivatives were first described by Stenhouse [1]. This type of reaction was used for the assay of furfural in food products by Winkler in 1955 [2]. In the Winkler method, furfural or hydroxymethylfurfural (HMF) is mixed with barbituric acid and *para*-toluidine to undergo a stepwise reaction. The basic Winkler method was modified for efficient assay of furfural and HMF in various food samples [3,4]. However, *para*-aminobenzoic acid was preferred more than *para*-toluidine (*para*-toluidine is a carcinogen) [3]. Many furan ring-opening reactions have been performed, and physical and optical properties of their products were studied [5–15]. In 2000, a Meldrum's activated furan (MAF) compound reacted with some cyclic secondary aliphatic amines to prepare a pair of products [5]. This type of reaction was studied again (in 2014) when a new class of T-type organic photochromic molecules named donor–acceptor Stenhouse adducts (DASAs) were prepared [6,7]. Various donors and acceptors were employed in this type of reaction [8,10,11,14,15]. Beside the studies, the analytical importance of the reaction type was also considered when MAF was grafted on amine-functionalized polycarbonate surfaces through DASAs formation reaction for colorimetric sensing of secondary amines in tetrahydrofuran (THF) [12]. Analytical assay using MAF was continued when appropriate amines were detected in THF, on solid supports and in gas phase [9]. The first example of amine sensing in aqueous solutions by employing this type of reaction was reported when poly (oxa-norbornene) backbones were used. The obtained limit of detection (LOD) for *n*-butylamine, diethylamine, indoline and *p*-methoxyaniline were 10, 20, 20 and 100 $\mu\text{g mL}^{-1}$, respectively [16]. A true efficient classical analytical approach for selective sensing of an amine in aqueous solutions based on the ring opening furan reaction has not been reported so far.

Mesalazine (MES) is a medicine which is used to cure Crohn's disease and inflammatory bowel disease. MES has been known as a powerful scavenger for reactive oxygen species. Thus, it has an important role in the pathogenesis of inflammatory bowel disease and impairment of neutrophil function. In addition, MES inhibits natural killer cell activity and antibody synthesis, and also affects the cyclooxygenase and lipoxygenase pathways. It is a safe drug with very few adverse effects and good tolerances [17,18]. Due to its medicinal importance, MES has been assayed employing high-performance liquid chromatography (HPLC) [19–21], electrochemistry [22–29], capillary electrophoresis [30,31], chemiluminescence [32] and spectrofluorometry [33–35]. However, the sensing methods suffer some difficulties and limitations on selectivity [24], sensitivity [24,32], limit of detection [19], speed of analysis [34] and cost [19–21,30,31].

Colorimetric methods are generally simple, cheap, and are widely accessible for quality control. However, the methods may suffer some drawbacks and limitations on sensitivity, selectivity, analytical time, accuracy, reproducibility, cost of the reagents and sample manipulation protocol (including heating, cooling, control of temperature, and extraction or clean-up steps) [36–39]. MES, as an aromatic amine, is diazotized and then, appropriately forms an azo dye to develop a colorimetric approach [36]. Some of the other types of MES colorimetric methods use vanillin and Folin-Ciocalteu reagent [36], alizarin red sulfonate and 1,2-

naphthoquinone-4-sulfonate [37], 7-chloro-4,6-dinitrobenzofuroxane [40] and 1,1-diphenyl-2-picrylhydrazyl radical (DPPH) [21]. Development of a colorimetric procedure for MES assay having low sample manipulation and cost, and with high sensitivity and selectivity is very important. In addition, simple and cheap preparation of an appropriate chromogenic reagent in order to develop an analytical method is highly desirable. Meldrum's acid is easily synthesized using a condensation reaction between malonic acid and acetone in the presence of acetic anhydride and sulfuric acid [41]. On the other hand, furfural, a well-known and cheap byproduct compound prepared from the acidic process of biomass, is a commercially available starting material for many useful syntheses [42]. Furfural condenses safely with Meldrum's acid in water at 70 °C in good yield to form MAF.

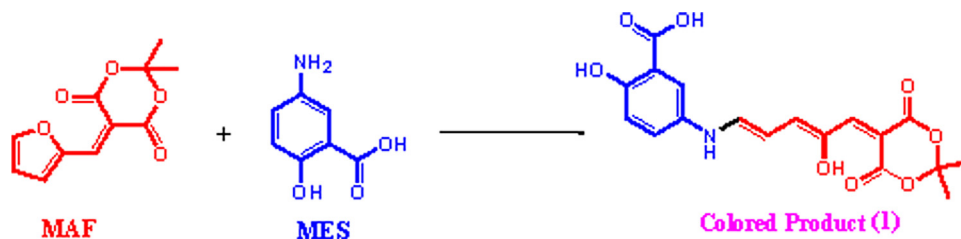
Through the last two decades, density functional theory (DFT) approach has been widely used to predict and explain some physical, chemical and biological properties of materials and biomaterials. DFT provides low cost computations and prepares reasonable results in comparison with the other *ab initio* methods [43]. Along with the widespread applications of DFT methods, time dependent DFT (TDDFT) approach has special importance for studying the excited states of molecules; especially vertical electronic excitations which are essentials for UV–Vis spectra [44].

The present work has studied the reaction of MES with MAF for understanding some spectrochemical properties of the formed colored product and analytical importance of the reaction. Along with the experimental studies, DFT and TDDFT calculations have been employed to study the vertical electronic excitations of the colored product. The affecting parameters on MES-MAF reaction were identified and then, the CCD method as a powerful chemometric approach has been applied to define a mathematical equation. According to the MES-MAF reaction in an aqueous mixture of Triton X-100 and sodium acetate, a colorimetric approach has been developed for sensing of MES in pharmaceuticals and water samples (Scheme 1). Important features of the method such as simplicity, sensitivity, selectivity, analysis time and economics have been investigated. The method is the first applicable and efficient furan ring-opening reaction based analytical method for assaying of a primary aromatic amine in aqueous media. The other furan ring-opening based methods have only been successful in detection of secondary amines in organic or gaseous samples [9,12].

2. Experimental section

2.1. Apparatus

UV–vis spectra were recorded by utilizing a Shimadzu double beam spectrophotometer model UV-1650 PC equipped with a pair of matched quartz cells with 10.0 mm path length (Hellma). Absorbances were measured at 575 nm by a single beam spectrophotometer Jenway model 6305. Structure of appropriate compounds were identified by ^1H NMR spectroscopy (INOVA-500) using DMSO d_6 as solvent. Chemical shifts were given in ppm (δ) relative to TMS as an internal standard. Coupling constants (J) were also reported in Hertz. Thin layer chromatography was carried out using commercially available Merck F254 aluminum backed silica plates. Melting points (un-corrected) were measured with a Stuart SMP-3 apparatus. Mass spectra were recorded with



Scheme 1. Reaction of MES with MAF.

an Agilent Technology (HP) 5973 Network Mass Selective Detector mass spectrometer operating at an ionization potential of 70 eV. Ultrasonic bath (Bandeline model Sonorex Digiplus DL 102H) was used to disperse and dissolve the reagents. Rotary vacuum evaporator (4011 Digital, Heidolph Company, Germany) and hotplate magnetic stirrer (Heidolph MR 3001 K) were also employed.

2.2. Reagents and solutions

THF, ethanol, hydrochloric acid, sodium acetate (NaOAc), sodium dodecyl sulfate (SDS), Triton X-100, furfural, barbituric acid, 2-thiobarbituric acid and 1,3-dimethylbarbituric acid were purchased from Merck (Germany). Cetylpyridinium chloride (CPC) and MES were purchased from Loba-Chemie (India) and Alfa Aesar (Germany), respectively.

Meldrum's acid was synthesized according to a previously reported procedure by a condensation reaction between acetone and malonic acid in acetic anhydride and sulfuric acid [41]. 5-(2-Furylmethylene)-2-thioxo-1,3-dihydropyrimidine-4,6-dione (TBAF), 5-(2-furfurylidene)barbituric acid (BAF), 5-(furan-2-ylmethylene)-1,3-dimethylpyrimidine-2,4,6(1H,3H,5H)-trione (DiBAF) and MAF (in Scheme 2) were synthesized according to the reported procedures [6,45,46]. Briefly, furfural (2 mmol) was added to a stirred aqueous solution of barbituric acid (2 mmol) or 2-thiobarbituric acid (2 mmol). After 5 min (1 hr in case of 2-thiobarbituric acid), the produced solids were isolated by a simple filtration and then, were dried [45,46]. For preparation of DiBAF, an aqueous dispersion of 1,3-dimethylbarbituric acid (10.5 mmol) was reacted with furfural (10 mmol) at room temperature (20 °C, 2 h). In case of MAF, reaction between Meldrum's acid (10.5 mmol) and furfural (10 mmol) was performed at 75 °C for 2 h. The crude DiBAF and MAF solid products were filtrated and washed with cold deionized water. Then, the solids were dissolved in CH₂Cl₂ and then, washed sequentially with a saturated aqueous solution of NaHSO₃, water, a saturated aqueous solution of NaHCO₃ and brine. Then, the organic layer was dried over CaCl₂ and filtered. Finally, the organic solvent (CH₂Cl₂) was evaporated to give DiBAF and MAF as the pure bright yellow powders [6].

Standard stock solution of 500 μg mL⁻¹ of MES was prepared in dilute hydrochloric acid. The fresh different concentrations of DiBAF and MAF were prepared in ethanol or THF by keeping sonication for 10 min. The solutions of the surfactants were prepared in deionized water.

All analytical experiments were carried out at room temperature. All of the other solvents and materials used were purchased from commercial suppliers and were used as received. Deionized water was used throughout all of the appropriate dilutions.

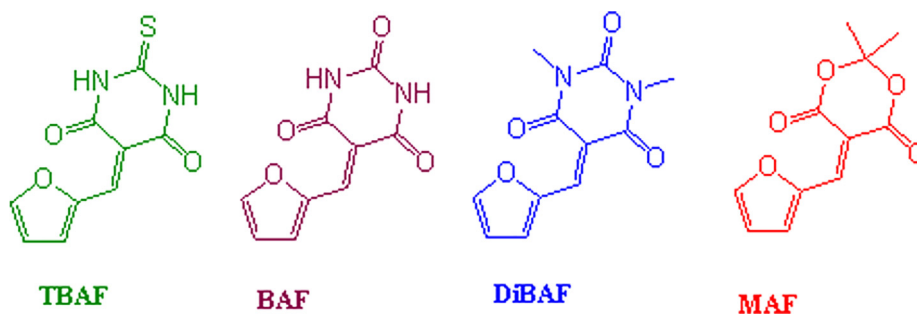
2.3. Analytical procedure

Sample solution (7.5 mL), 150 μL of NaOAc 2.0 mol L⁻¹, 1.5 mL of Triton X-100 aqueous solution (20.0%, wt/v) and 0.5 mL of MAF solution in ethanol (4.0 × 10⁻² mol L⁻¹) were added to a 10 mL volumetric flask. The reaction mixture was made up to the mark with deionized water. The solution was allowed to stand for 10 min at room temperature prior to absorbance measurement at 575 nm against the appropriate blank (in the absence of MES). The net absorbance was used to assay MES by using the appropriate calibration equation.

2.4. Sample preparations

Four tablets (equivalent to 500 mg of MES in each tablet) were weighed and their average weight was estimated and ground to a homogeneous fine powder in a mortar. A quantity of powder equivalent to 100 mg of the drug was transferred to a 50 mL volumetric flask and dissolved in 20 mL of 0.1 mol L⁻¹ HCl by ultrasonication for 30 min. The solution was filtered, and the filter paper was washed with 10 mL of 0.1 mol L⁻¹ HCl. The solution was added to the filtrate and the final volume was made up to 50 mL with deionized water [23]. After appropriate dilution, the analytical procedure was obeyed.

Tap, lake and river water samples were collected from Ardabil tap water, Shorabil Lake and Baliqly Chay river. All of the water samples were immediately filtered by Whatman filter paper no. 40 before use.



Scheme 2. Chemical structures of TBAF, BAF, DiBAF and MAF.

2.5. Central composite design (CCD) analysis

The MINITAB statistical package (Minitab Inc. Release 17.0) software was employed for data analysis and corresponding diagram plotting.

3. Results and discussion

3.1. Characterization of the colored product

According to previously reported results on the reaction between MAF and amines [5–15], it is expected that the colored compound **1** could be formed by the reaction of MES and MAF. Fig. 1 displays the proposed mechanism for this transformation. The reaction starts with the nucleophilic attack of MES to MAF to form the intermediate **I** [47,48]. This intermediate undergoes ring opening reaction to produce the intermediate **II**. Intramolecular proton transfer in the intermediate **II** generates the colored product **1**. The loss of color over time can be attributed to the cyclization of the colored molecule **1** [1]. Accordingly, compound **1** undergoes intramolecular cyclization over time to produce a colorless compound **2** [49].

Since the reaction of primary anilines and primary aliphatic amines with MAF produces unstable and inseparable products [6], the formation of colored compound **1** and colorless compound **2** is confirmed by examining the ^1H NMR spectrum of the mixture of MES and MAF in deuterated DMSO. For this purpose, both of the MAF and MES were mixed together in deuterated DMSO. Then, ^1H NMR spectroscopy was carried out in the first 5 min and also after one hour. Fig. 2b depicts some significant ^1H NMR signals of the MES-MAF mixture within the first 5 min and also after 1 h reaction. The e, f, g, h and OH-enol signals are attributed to the colored compound **1**, while the i, j, k, l and m signals can be related to the colorless cyclic form **2** [50]. As shown in Fig. 2b, the integrals of the NMR signals of the compound **2** within the first 5 min are negligible, but after one hour the signals associated with the compound **2** increase. These observations are consistent with the changes in the UV-vis spectrum of the MES-MAF mixture over time. This change in UV-vis absorption spectrum (Fig. 2a) can be attributed to the conversion of the colored compound **1** to the colorless cyclic form **2**. The formation of the expected products was also confirmed by employing the mass spectrometric analysis (Fig. S3).

3.2. Results of DFT studies

The possible structures of the colored product **1** obtained from the reaction between MAF and MES were optimized by DFT method. Accordingly, ωB97 functional with long range (LC) and exact local exchange corrections were applied with 6-31++G (3df,3pd) basis set [51–53]. For all calculations, the GAMESS quantum chemistry program was applied [54]. After a gas phase optimization, the calculations were continued in the solution using the polarizable continuum model containing integral equation formalism (IEFPCM) in conjunction with the solvation model based on density (SMD) approach in DMSO and water as solvents [55,56]. Three different structures of product **1** (Fig. 3) were considered for the computational studies. As can be seen, A and B forms are tautomers of each other, and A and C forms are conjugated acid-base forms. The optimized structures of these molecules are presented in Fig. 4. After that, time dependent density functional theory (TDDFT) was exerted to study the vertical excitations of the forms [57]. Table 1 shows the complete obtained results as brief. Also, the highest occupied molecular orbital (HOMO) and the lowest unoccupied molecular orbital (LUMO) of these different forms of product **1** are shown in Table 2. Further, in order to determine the types of the electronic excitation (local or charge transfer), the wavefunctions of these forms were analyzed by Multiwfn program [58].

MES and sulfasalazine are two compounds containing salicylic acid moieties. The compounds show pK_a s related to $-\text{COOH}$ acidic groups on their salicylic acid moieties as 2.30 and 2.81 in water at 25 °C, respectively [59,60]. According to the pK_a s, the compounds in aqueous solutions are present preferably as anions (salicylate). Product **1** has a salicylic acid moiety similar to those of MES and sulfasalazine. Thus, product **1** is strongly accepted to be present as an anion in aqueous sodium acetate solution (form C). In addition, salicylic acid has a dissociation constant (pK_a) equal to 6.6 in DMSO [61]. Thus, product **1** in DMSO is strongly accepted as form A. On the other hand, the basic concepts of hydrogen transfer in tautomerism predict that hydrogen transfer from nitrogen of MES moiety to oxygen of Meldrum's acid moiety in product **1** has low probability [62,63]. According to the statements, the most possible forms of product **1** in DMSO and sodium acetate aqueous solutions are form A and form C, respectively.

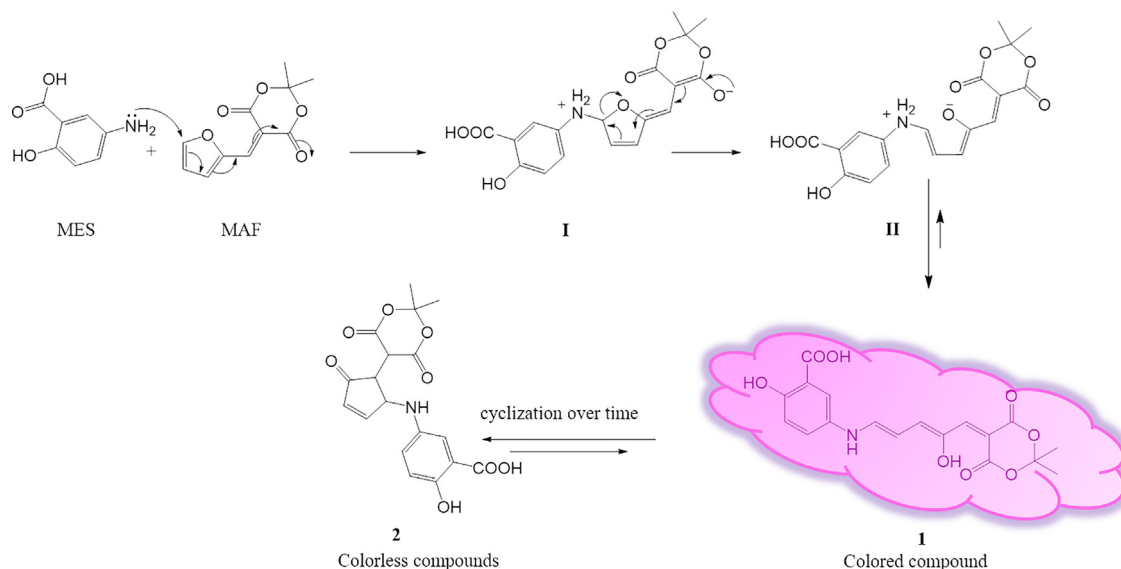


Fig. 1. The proposed mechanism for the formation of compound **1** and **2** through the reaction between MES and MAF.

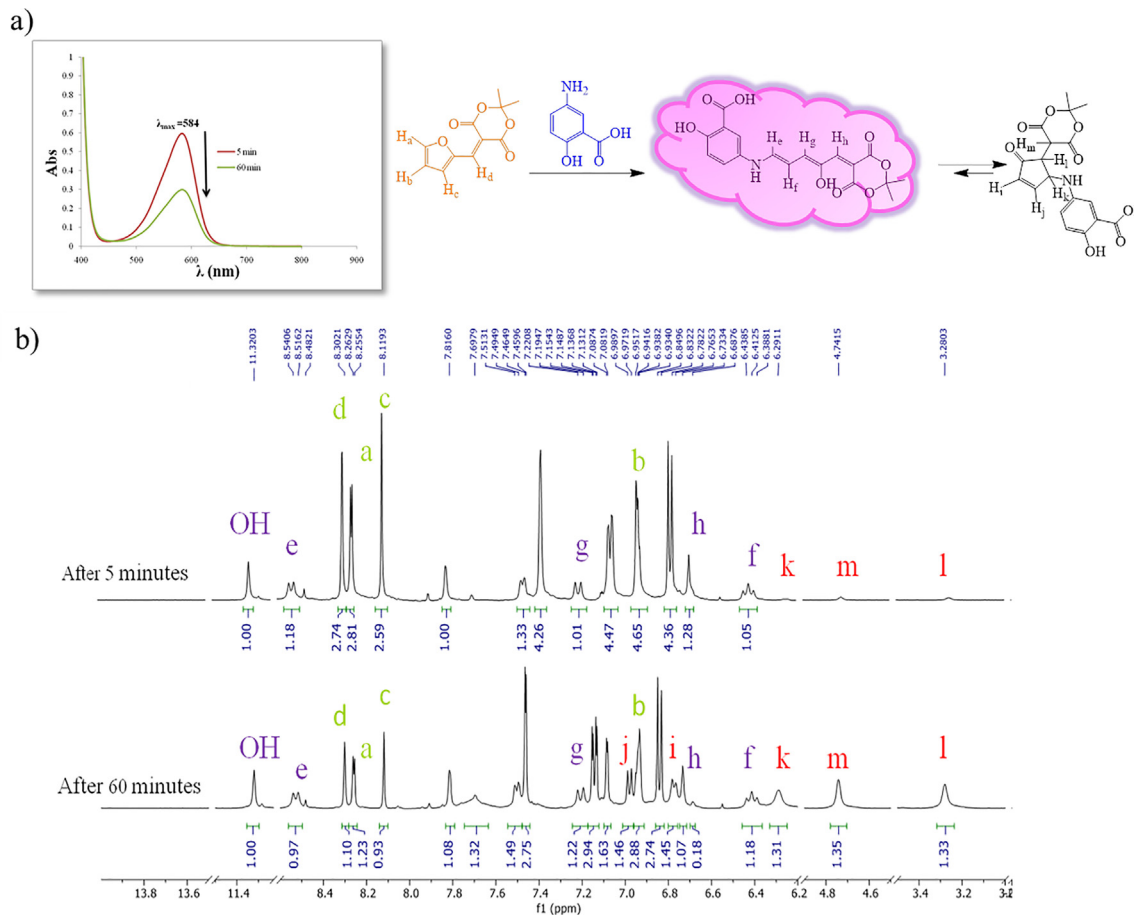


Fig. 2. Reaction with time: a) Absorption spectra of MES-MAF mixture after 5 and 60 min in DMSO and b) ^1H NMR spectra of MES-MAF mixture after 5 and 60 min in DMSO d_6 .

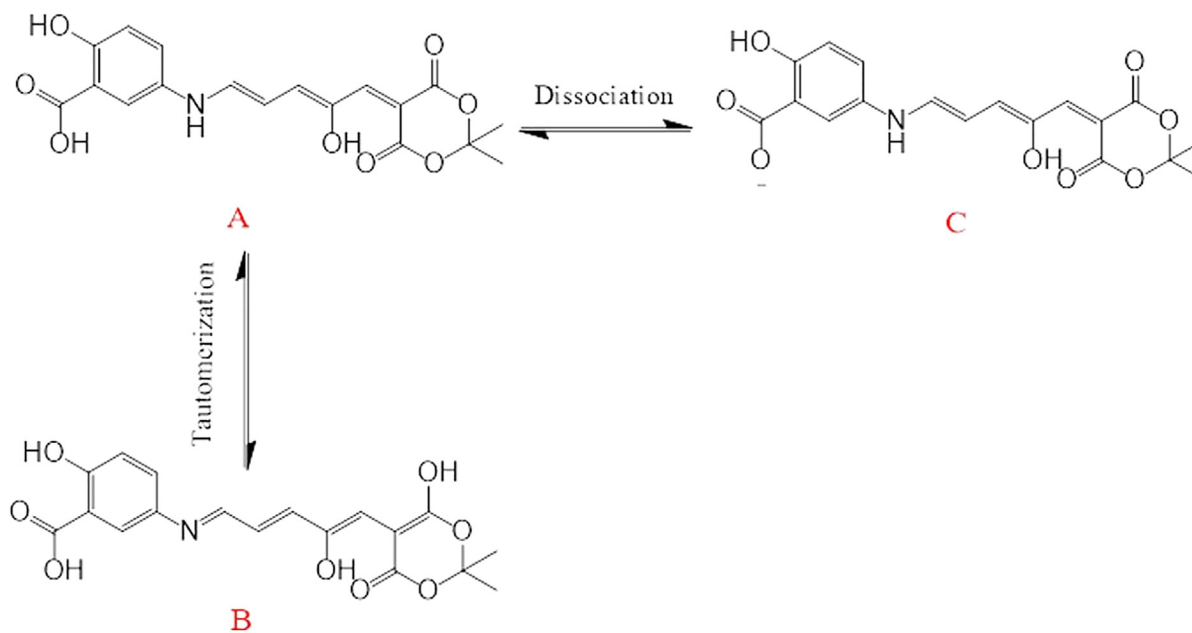


Fig. 3. Considered different forms of product 1.

The results obtained by the TDDFT analysis in DMSO including the length of charge transfer (LCT) through the electronic excitation from HOMO to LUMO are also reported in Table 1. The dis-

tance for charge transfer of form A is shorter than a normal C=C bond length of this form (1.37 Å). Thus, it is concluded that excitation of this form at λ_{max} does not exhibit a charge transfer charac-

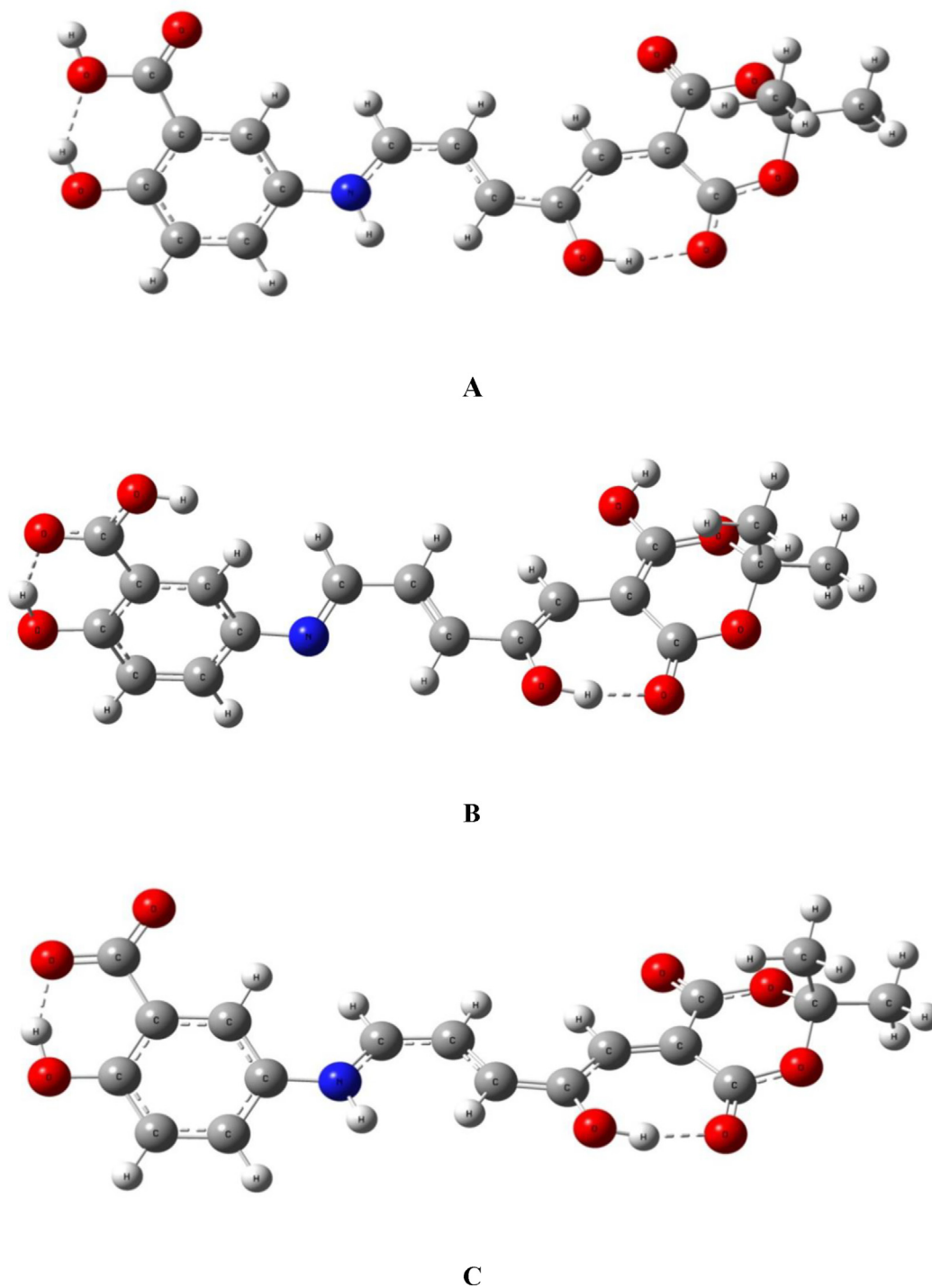


Fig. 4. The optimized structures of product **1** in different forms (A–C).

Table 1

Details of TDDFT calculations results for different forms of product **1** (A–C).

Molecule	Calculated λ_{\max} (nm)	f	μ_g (Debye)	μ_e (Debye)	transition	LCT (Å)
A ^D	490.7	1.1511	4.88	15.30	HOMO(π) \rightarrow LUMO(π^*)	0.382
B ^D	332.1	1.0370	15.89	21.78	HOMO(π) \rightarrow LUMO(π^*)	2.397
C ^D	526.8	1.1850	28.89	20.69	HOMO(π) \rightarrow LUMO(π^*)	2.525
C ^W	508.9	1.1970	29.02	21.34	HOMO(π) \rightarrow LUMO(π^*)	0.978

A^D–C^D: the results obtained for different forms of product **1** in DMSO.

C^W: the results obtained for form C in water.

f is the oscillator strength; μ_g is dipole moment of the ground state; μ_e is dipole moment of the excited state.

Table 2
Orbital structures of HOMOs and LUMOs for different forms of product 1.

Form	HOMO	LUMO
A ^D		
B ^D		
C ^D		
C ^W		

A^D-C^D: the shapes of HOMOs and LUMOs obtained for different forms of product 1 in DMSO.
C^W: the shape of HOMO and LUMO obtained for form C in water.

teristic and it is taken place a local $\pi \rightarrow \pi^*$ excitation. However, form B can exist in DMSO with LCT larger than C=C bond length through N=C=C moiety, see Tables 1 and 2. Therefore, the charge transfer can occur only in a form with less possibility (form B). The shapes of HOMO and LUMO for form B in Table 2 confirm the fact. Otherwise, in DMSO both LCTs and the shapes of HOMOs and LUMOs in Tables 1 and 2, confirm the charge transfer property of the excitations for form B and form C.

Beside the shapes of HOMO and LUMO in Table 2, form C shows a LCT less than 1.37 Å (in Table 1) in water. Thus, there is not charge transfer property for the excitation.

3.3. Study on absorption spectra

Four different reagents from the group of activated furans (TBAF, BAF, DiBAF and MAF) were synthesized [6,45,46] and tested for reaction with MES. Preliminary experiments showed that TBAF and BAF could form colored products with MES, but their solubilities in aqueous micellar solutions, THF and ethanol were insufficient to develop a MES sensing method. In establishment of a spectrophotometric procedure, solubility of the reagents and products in the final solution is essential. Thus, TBAF and BAF were not considered for further studies.

The other reagents (DiBAF and MAF) were also tested. The reagents formed colored products with MES having sufficient solubility in the aqueous micellar solutions, THF and ethanol. Thus, DiBAF and MAF were considered for further investigations.

Also, the tests showed that the presence of surfactants in the media increases the absorbance of the solutions and offers more stability for the formed products. Figs. 5–7 display the spectra of the solutions (sample and blank) together with time correlation of the measured absorbances. The surfactants applied were SDS (an anionic surfactant), Triton X-100 (a non-ionic surfactant) and CPC (a cationic surfactant). According to the spectra in Fig. 5, it is observed that MAF causes more sensitivity than DiBAF in SDS

media (at their λ_{\max}). Also, Fig. 6 shows that in Triton X-100 solutions, the colored product of MES-MAF reaction was more stable than that of MES-DiBAF reaction. In Triton X-100 media, MAF and DiBAF showed the same sensitivity, but less blank signal was observed for MAF. Fig. 7a showed that the spectra of the sample and blank solutions related to DiBAF reagent in CPC media were the same. In CPC, MAF reacted with MES and formed a yellow colored solution (a shoulder was observed in the UV-vis spectrum of the sample and no λ_{\max} was observed). As we know, colorimetric measurements at λ_{\max} offer some advantages on sensitivity, calibration linearity and selectivity [64]. The net absorbance of the sample solution was obtained at 431 nm in CPC media (inset graph in Fig. 7b). The inset graph showed that the absorbance was increasing with time (the kinetics of the MES-MAF reaction was slow). Such the slow reaction kinetic causes limitation on the speed of analysis.

The series of experiments compared different chromogenic reagents and surfactants to make a decision on selecting the most efficient chromogenic reagent and surfactant. For further experiments, MAF and Triton X-100 were selected as the best chromogenic reagent and surfactant, respectively.

The photoswitching reactions of the colored Stenhouse adducts depend on the nature and composition of the solutions [6,7,42,50]. Therefore, the effect of light on MAF-MES reaction in Triton X-100 solutions was studied. Fig. 8 depicts the results of the experiments. As can be seen, the sensitivity of the method does not depend on the presence or absence of laboratory light during the experiments.

3.4. Univariate optimization method

In addition to the univariate method, many chemometric methods have been applied for optimization in analytical chemistry. The methods process some experimental results using a computer program to predict the optimum condition. The effects of parameters on the analytical response are presented as an equation for some of

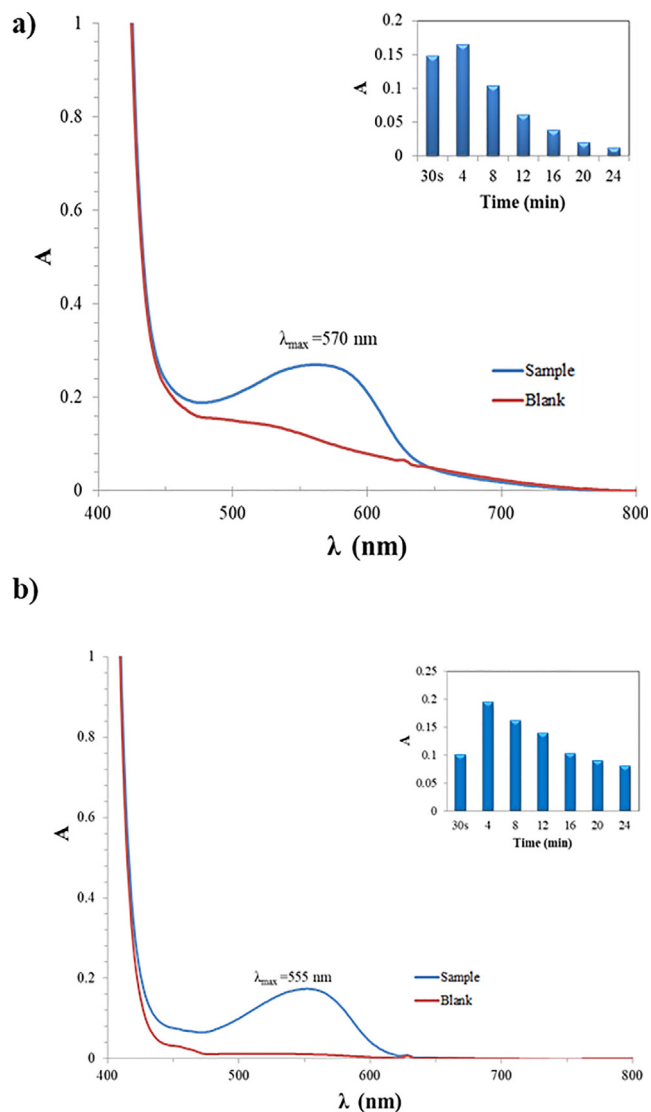


Fig. 5. Absorption spectra of the manipulated MES containing solutions in SDS media using a) DiBAF and b) MAF. Condition: chromogenic reagent 1.0 mmol L⁻¹, SDS 1.0% (wt/v), MES 20.00 μg mL⁻¹, THF 10% (v/v) and NaOAc 0.02 mol L⁻¹.

the chemometric approaches. In this research, both the central composite design (CCD) optimization method and the univariate method were used to optimize the condition of the MES detection system. The results obtained by the univariate method prepared some information about the relationship between the sensitivity and the effective parameters. Also, the results of the univariate optimization method were applied to define the ranges of the parameters that must be considered during applying the CCD optimization method. The univariate optimization method was applied step by step. Every experiment was performed three times. The absorbance was monitored at 575 nm when concentration of Triton X-100 as the solubilizing and stabilizing agent was varied. The results of the experiment are shown in Fig. 9a. As can be seen, the best sensitivity was obtained when Triton X-100 had a concentration of 2.0% (wt/v). Thus, 2.0% (wt/v) was selected as the optimum concentration of Triton X-100.

The concentration of MAF was changed and absorbance was detected. The results in Fig. 9b show the dependency of absorbance on the MAF concentration. The results show that the optimal concentration of MAF was 2.0 mmol L⁻¹.

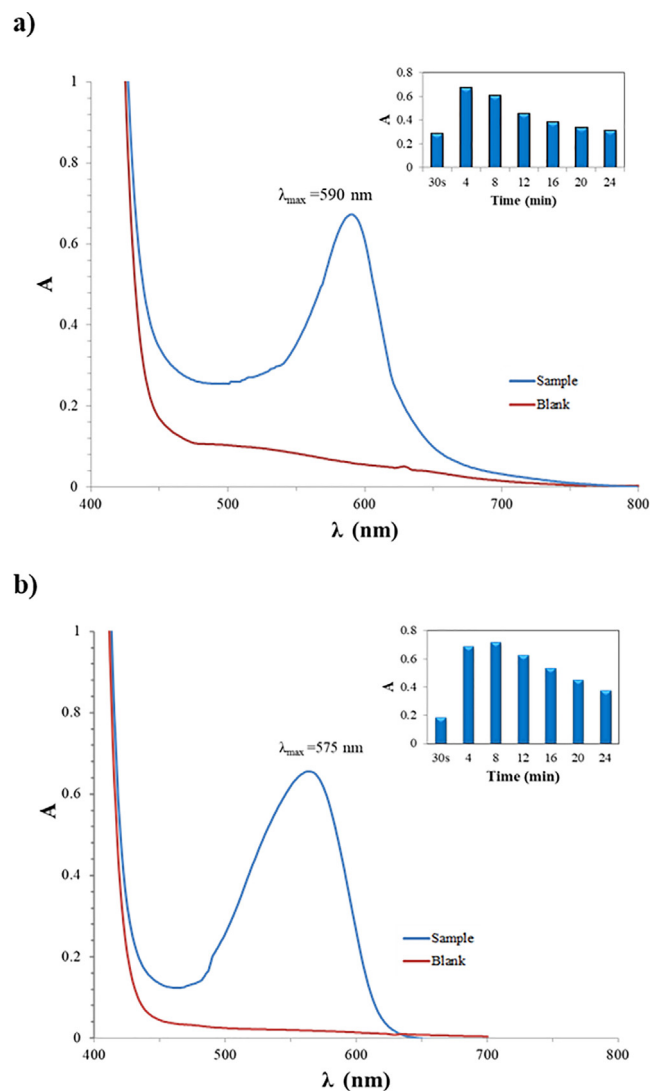


Fig. 6. Absorption spectra of the manipulated MES containing solutions in Triton X-100 media using a) DiBAF and b) MAF. Condition: chromogenic reagent 1.0 mmol L⁻¹, Triton X-100 1.0% (wt/v), MES 20.00 μg mL⁻¹, THF 10% (v/v) and NaOAc 0.02 mol L⁻¹.

NaOAc as the major constituent in the final solution not only normalizes matrix of the solution but also controls the pH of the solution. The concentration of NaOAc was varied and the sensitivity was investigated. The obtained results in Fig. 9c show that 0.030 mol L⁻¹ of NaOAc caused the best sensitivity. Thus, 0.030 mol L⁻¹ of NaOAc was chosen for the next optimization steps.

THF has been used as co-solvent in preparation of the stock solution of MAF. Thus, THF is present in the final solution prior to the measurement of absorbance. Ethanol as a common water miscible solvent was also examined in the preparation of the MAF stock solution. Different volumes of ethanol or THF were added to the final solution, separately, while the final concentration of MAF was constant (2.0 mmol L⁻¹). The results have been shown in Fig. 10a. The results show that the sensitivity is inversely dependent on the volume of the organic solvent added. The results also reveal that ethanol offers more sensitivity against THF. Thus, the lowest possible volume of ethanol (0.5 mL) was selected for further experiments.

The reaction period between MAF and MES was changed and absorbance was monitored. The results of the study are given in

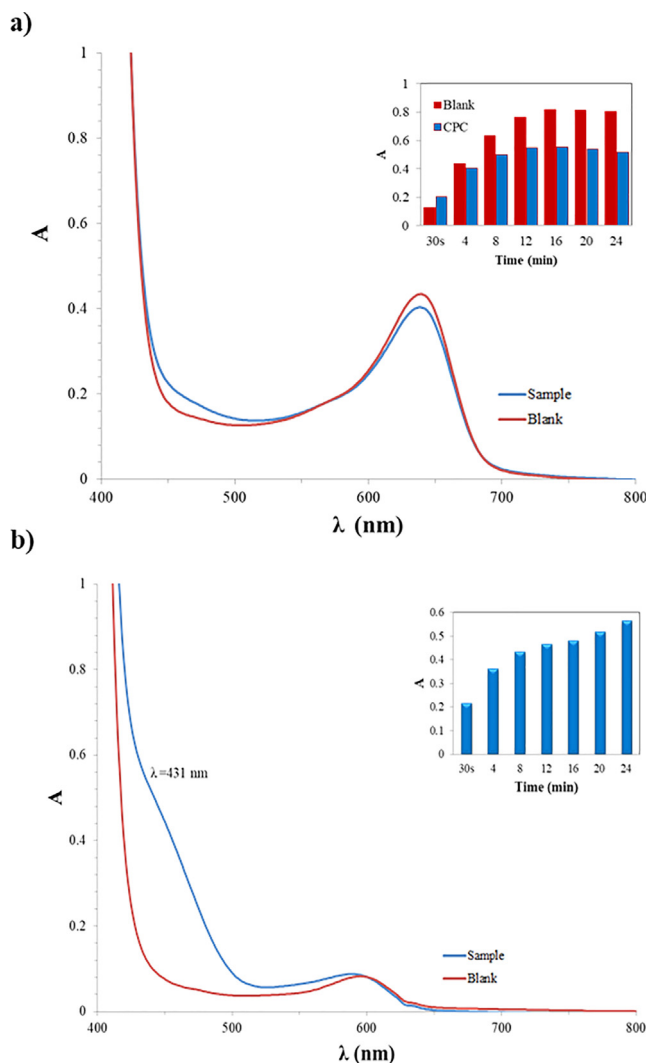


Fig. 7. Absorption spectra of the manipulated MES containing solutions in CPC media using a) DiBAF and b) MAF. Condition: chromogenic reagent 1.0 mmol L⁻¹, CPC 1.0% (wt/v), MES 20.00 μg mL⁻¹, THF 10% (v/v) and NaOAc 0.02 mol L⁻¹.

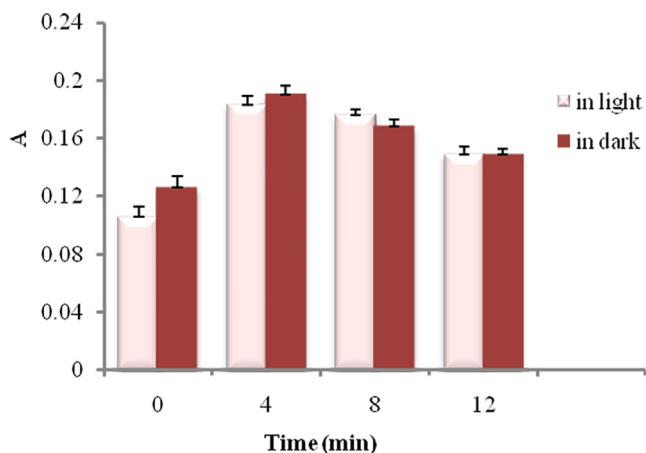


Fig. 8. Effect of light on the absorbance of the solution. Condition: MAF 0.5 mmol L⁻¹, Triton X-100 1.0% (wt/v), MES 10.00 μg mL⁻¹, THF 10% (v/v) and NaOAc 0.01 mol L⁻¹ at room temperature.

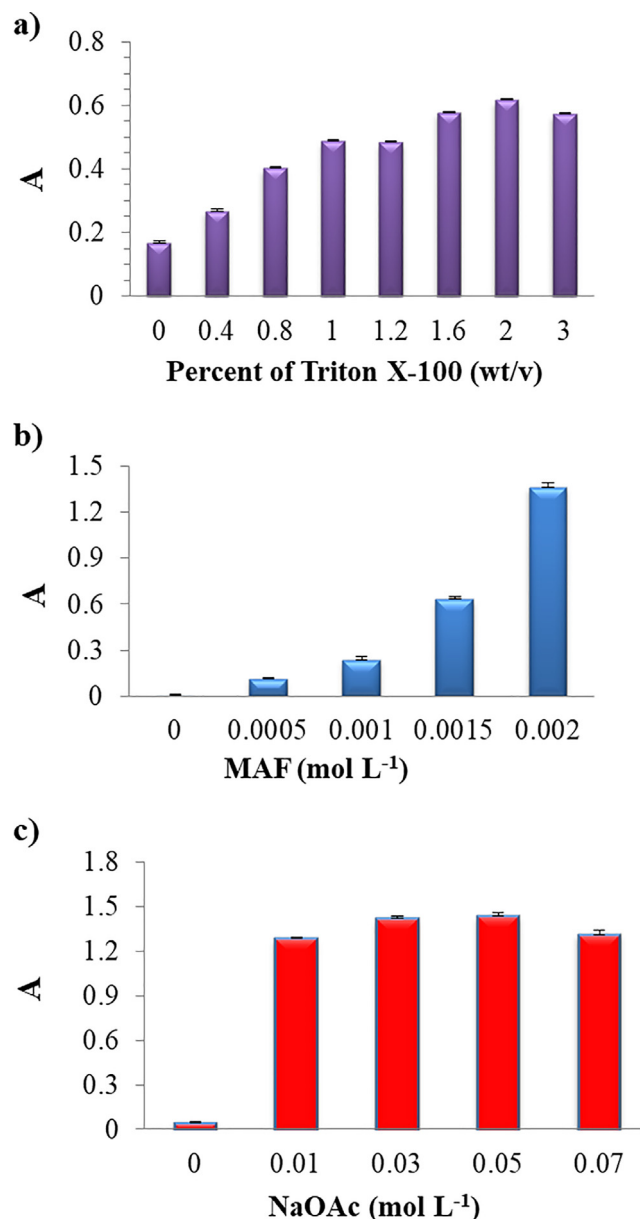


Fig. 9. Effect of: a) Triton X-100, b) MAF and c) NaOAc on the sensitivity of the method. Condition for (a): MES 17.5 μg mL⁻¹, NaOAc 0.04 mol L⁻¹, MAF 1.5 mmol L⁻¹, THF 10% (v/v) and reaction period of 6 min. Conditions were consecutively changed for the study of the other parameters according to the univariate optimization method.

Fig. 10b. As seen, the greatest sensitivity has been attained after 10 min.

A 10 min reaction period was considered and the effect of ionic strength was investigated. The results in Fig. 10c showed that the lowest ionic strengths caused the greatest sensitivity.

3.5. CCD method for studying MES-MAF reaction

In order to evaluate the dependence of absorbance on the affecting factors and to understand how the parameters interact with each other, the CCD chemometric method was applied. The modeling was established for three factors involving five levels [65].

The involved factors with the true and encoded quantities at diverse levels are shown in Table S1. A fixed concentration of

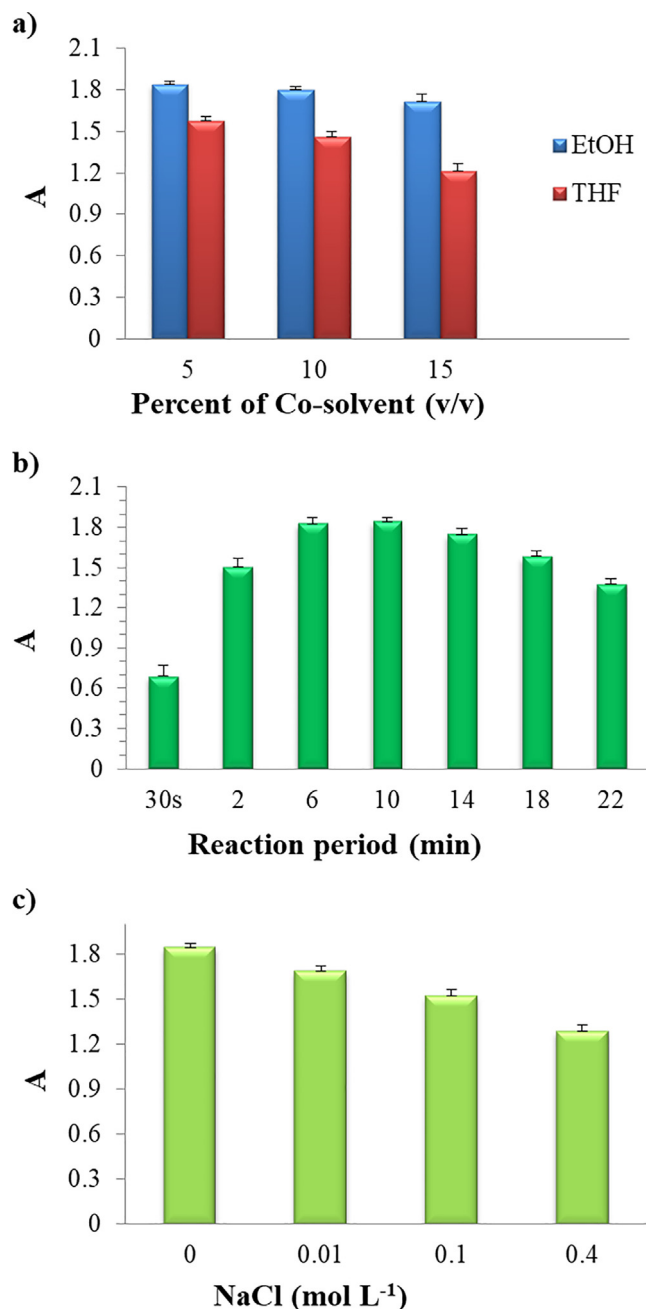


Fig. 10. Effect of: a) Co-solvent, b) Reaction period and c) NaCl on the sensitivity of the method. Condition for (a): MES 17.5 $\mu\text{g mL}^{-1}$, NaOAc 0.03 mol L^{-1} , MAF 2.0 mmol L^{-1} , Triton X-100 2.0% (wt/v) and reaction period of 6 min. Conditions were consecutively changed for the study of the other parameters according to the univariate optimization method.

MES (8.75 $\mu\text{g mL}^{-1}$) was used through all the experiments. Table S2 lists the CCD matrix in 39 experimental runs for these variables and responses. The results of the analysis of variance (ANOVA) and P-values by the CCD optimization procedure are presented in Tables 3 and 4. The polynomial equation which describes the absorbance of the solution in terms of significant variables is:

$$A = \text{Constant} - \beta_1 X_1 + \beta_2 X_2 + \beta_3 X_3 - \beta_{11} X_1^2 - \beta_{22} X_2^2 + \beta_{12} X_1 X_2 - \beta_{13} X_1 X_3 + \beta_{23} X_2 X_3 \quad (1)$$

The ANOVA results in Tables 3 and 4 revealed that the model is highly significant. The good predictability of the model shows that

the lack of fit is insignificant. The value of determination coefficient ($R^2 = 0.8585$) also indicated that the fitting is well. Finally, based on ANOVA, the reliability of the model was concluded. According to Equation (1), X_1 , X_2 and X_3 factors linearly affect the response. Also, the squares of X_1 and X_2 are significant. In addition, it was found that the interactions of X_1 , X_2 , and X_3 with each other affect the response. Three-dimensional response surfaces in Fig. 11 clearly illustrate the obtained outcomes. CCD predicted the optimal values of time, and Triton X-100 and MAF concentrations. They were 10.0 min, 3.0% (wt/v) and $2 \times 10^{-3} \text{ mol L}^{-1}$, respectively.

MES at the concentration of 8.75 $\mu\text{g mL}^{-1}$ was selected and two series of experiments were conducted. Initially, the univariate optimization condition was applied. The measured absorbance was 0.710 ± 0.034 ($n = 8$). Also, some measurements were conducted when the condition proposed by the CCD method was applied. The measured absorbance was 0.890 ± 0.031 ($n = 8$). The paired t -test at 95% confidence interval confirmed the presence of a significant difference between the means of the both results. Thus, the condition proposed by the CCD method was selected to be employed in the subsequent experiments.

3.6. Analytical characteristics

The optimized condition (obtained by the CCD approach) was applied and important analytical features of the method were evaluated. Initially, different concentrations of MES were prepared, the procedure was obeyed and the absorbance of the solutions was measured at 575 nm. A linear calibration plot was obtained within the wide range of 0.06–9.30 $\mu\text{g mL}^{-1}$ (Fig. S4).

To obtain the precision and accuracy of the method, different concentrations of MES at 0.70, 1.00 and 8.40 $\mu\text{g mL}^{-1}$ were tested. Also, the reproducibility of the method for 1.00 $\mu\text{g mL}^{-1}$ of MES was investigated.

The minimum concentration of MES that can be detected (LOD) is another important analytical index. LOD was obtained 0.04 $\mu\text{g mL}^{-1}$ of MES when ten times repetitive analysis of blank was performed. The important analytical characteristics of the method are given in Table 5. Therefore, the satisfactory efficiency of the MES sensing approach is validated.

3.7. Selectivity of the method

The effects of different species on the detection of MES were investigated under optimum experimental conditions when the other species were added individually. MES concentration was 2.00 $\mu\text{g mL}^{-1}$ in all of the experiments. A specie was considered as an interferer when it caused $\geq 5\%$ error on the MES concentration. The results in Table 6 indicated that the frequently added cations, anions and organic chemicals did not interfere at 200-fold (wt/wt) ratio. In addition, some pharmaceutical amines such as procaine, procainamide, metoclopramide, sulfamethazine and dapson were also tested. The results showed that the pharmaceutical amines did not cause considerable interferences on the MES detection.

3.8. Sample analysis

Various pharmaceutical samples and three different water samples were tested to evaluate the applicability of the MES detection method. In the analysis of water samples, 5.0 mL of the water samples (after filtration with Whatman filter paper no. 40) were employed. The results of the study are reported in Table 7. MES was not found in the water samples. Thereafter, the water samples were spiked with two different concentrations of MES (1.0 and 5.0 $\mu\text{g mL}^{-1}$) and were analyzed ($n = 6$) according to the analytical procedure. The obtained recoveries and relative standard devia-

Table 3
Analysis of variance for the experiments in Table S2.

Source	DF ^a	AdjMS ^b	F ^c	P ^d
Model	10	0.157415	24.05	0.000
Blocks	1	0.028042	4.29	0.048
Linear	3	0.430996	65.86	0.000
Square	3	0.043242	6.61	0.002
Interaction	3	0.039551	6.04	0.003
Residual error	27	0.004259	–	–
Lack-of-fit	18	0.005324	2.17	0.199
Pure error	10	0.006544	–	–
Total	38	–	–	–
R ²	0.8585	–	–	–

^a Degree of freedom;^b Adjusted mean of squares;^c F test;^d Probability value.**Table 4**
Analysis of variance (coded coefficients).

Term	Coefficient	SE Coefficient ^a	T-value ^b	P-value ^c
Constant	0.4281	0.0233	18.35	0.000
X ₁	−0.0099	0.0166	−0.60	0.556
X ₂	0.1302	0.0155	8.41	0.000
X ₃	0.1741	0.0155	11.25	0.000
X ₁ X ₁	−0.0492	0.0166	−2.97	0.006
X ₂ X ₂	−0.0473	0.0152	−3.12	0.004
X ₃ X ₃	−0.0281	0.0152	−1.85	0.075
X ₁ X ₂	0.0425	0.0202	2.10	0.045
X ₁ X ₃	−0.0459	0.0202	−2.27	0.031
X ₂ X ₃	0.0592	0.0202	2.93	0.007

^a Standard error;^b t-statistics;^c Probability value.

tions (RSDs) were in the ranges of 96.0–105.0 % and 1.9–5.2%, respectively (Table 7). Different pharmaceutical tablets were also analyzed. The results in Table 8 show satisfactory accuracy and reproducibility of the method. The recovery of the method was in the range of 99.3–102.3 %.

3.9. Comparison with the other spectroscopic MES sensing methods

The characteristics of the simple MES sensing method should be compared with some of the previously reported methods to define its analytical efficiency. The efficiency of the presented method has been compared with some spectroscopic methods in Table 9. The methods show some limitations on cost [21,37,40], simplicity (condition must be precisely controlled) [36,66], LOD [37,40,66] and linear dynamic range (LDR) [21,40]. The presented method can be easily employed in a general laboratory for MES detection in pharmaceutical and polluted water samples. In this method,

Table 5
Analytical characteristics of MES assay method.

Slope of calibration curve	0.128
Intercept of calibration equation	0.006
Square of correlation coefficient (R ²)	0.9981
Limit of detection (μg mL ^{−1})	0.04
Linear dynamic range (μg mL ^{−1})	0.06–9.30
Repeatability (RSD%) ^a :	
0.70 μg mL ^{−1}	3.2
1.00 μg mL ^{−1}	2.5
8.40 μg mL ^{−1}	0.6
Recovery ^a :	
0.70 μg mL ^{−1}	96.3
1.00 μg mL ^{−1}	98.9
8.40 μg mL ^{−1}	100.8
Reproducibility (RSD%) ^b :	
1.00 μg mL ^{−1}	3.5
Recovery ^b :	
1.00 μg mL ^{−1}	100.6

± Amounts are standard deviations.

^a For 8 replicate measurements;^b For 7 day period;**Table 6**
Influence of foreign species on the detection of 2.0 μg mL^{−1} MES.

Foreign species	(Wt _{species} /Wt _{MES})
Mg(II), Ca(II), Ni(II), Fe(III), K(I), Na(I), Cl [−] , SO ₄ ^{2−} , H ₂ PO ₄ , NO ₃ [−] , Serine, Glycine, Alanine, Methionine, Glutamic acid, Leucine, Asparagine, Sucrose, Citrate, Procaine, Procainamide, Metoclopramide	200 ^a
Sulfamethazine, Glucose	200
L-Cysteine	100
Dapsone	50

^a The maximum tested concentration. The ratio did not show any interference in the mentioned level.**Table 7**
Detection of MES in water samples.

Sample	MES, μg mL ^{−1} (n = 6)		Recovery, %
	Taken	Found	
Tap water	–	ND ^a	–
	1.00	0.96 ± 0.05	96.0
River water	–	ND ^a	–
	1.00	1.02 ± 0.03	102.0
Lake water	–	ND ^a	–
	1.00	1.03 ± 0.02	103.0
	5.00	5.25 ± 0.18	105.0

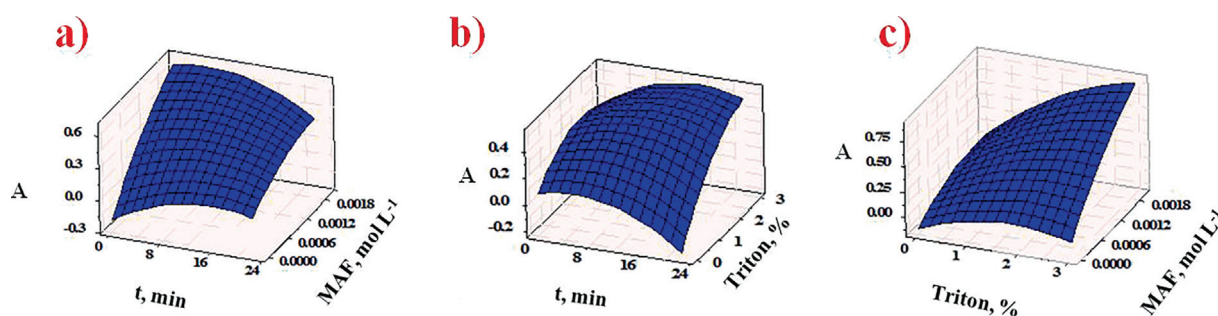
^a Non-determinable; ± Amounts are standard deviations.**Fig. 11.** Three-dimensional (3D) response surfaces obtained based on the model for optimization of chemical variables.

Table 8
Analysis of MES in pharmaceutical preparations.

Sample	Amount, mg tablet ⁻¹ (n = 4)		Recovery, %
	Taken	Found	
Sample 1 ^a	500	497 ± 2	99.4
Sample 2 ^b	500	511 ± 6	102.2
Sample 3 ^c	500	505 ± 9	101.0

± Amounts are standard deviations.

^a Tablet (500 mg); Iran hormone company; average mass of each tablet was 0.657 g.

^b Tablet (500 mg); Chemidarou company; average mass of each tablet was 0.773 g.

^c Tablet (500 mg); Arya company; average mass of each tablet was 0.698 g.

Table 9
Comparison of the MES analytical method with the other spectroscopic methods.

Characteristics of method	λ_{\max} , nm	LDR ^a , $\mu\text{g mL}^{-1}$	LOD ^b , $\mu\text{g mL}^{-1}$	Samples	Ref.
Colorimetry-uses DPPH radical	517	0.4–3	–	Tablet	[21]
Colorimetry-uses Folin-Ciocalteu reagent	655	1–30	0.004	Tablet	[36]
Colorimetry-uses a Diazo-coupling reaction	510	1–15	0.006	Tablet	[36]
Colorimetry-uses a Schiff base formation reaction	395	2–30	0.021	Tablet	[36]
Colorimetry-uses ARS reagent	600	15–98	4.92	Tablet	[37]
Colorimetry-uses NQS reagent	470	2–22	0.56	Tablet	[37]
Colorimetry-uses 7-Chloro-4,6-dinitrobenzofuroxane	500	0.32–4.6	0.3	Urine	[40]
Colorimetry-FIA ^c - uses o-coumaric acid	659	5–150	1.48	Tablet	[66]
Fluorimetry-uses N/P-doped carbon dots	487 ^d	0.076–19.9	0.02	Tablet, Blood	[67]
Colorimetry-uses MAF reagent	575	0.06–9.3	0.04	Tablet, Water	This work

^a Linear dynamic range;

^b Limit of detection; DPPH: 1,1-Diphenyl-2-picrylhydrazyl; ARS: Alizarin red sulfonate; NQS: 1,2-Naphthoquinone-4-sulfonate;

^c Flow injection analysis;

^d Emission wavelength.

MAF is employed as a chromogenic reagent. MAF can be simply prepared from furfural (a biomass derived reagent) as a starting material.

4. Conclusions

Easy preparation of a chromogenic reagent from the natural compounds for developing an analytical method is an advantage. A simple, sensitive and selective colorimetric method was developed for MES sensing based on the coupling of MES with MAF. The major reagent in the preparation of MAF was furfural (a biomass derived reagent). The obtained NMR spectra at different times revealed that the colored product was being converted to a colorless isomer. The optimum condition obtained by the univariate optimization method was employed to attain the best sensitivity. Besides applying the univariate method, the CCD method was employed to obtain the dependency of the method sensitivity on the affecting parameters. The CCD model was employed to discuss the effects of the reaction parameters on the sensitivity of the method. The study revealed that the response has been linearly dependent to the concentrations of Triton X-100 and MAF. Furthermore, squares of the reaction period and Triton X-100 had negative effects on the response. Also, the analytical response was dependent on $X_1 X_2$, $X_1 X_3$ and $X_2 X_3$. The efficiencies of the optimum conditions attributed to the CCD and univariate methods were compared with each other and the optimum condition proposed by the CCD method was chosen due to greater sensitivity.

DFT calculations were employed on three possible structures attributed to the colored product. Neutral and anionic forms are the most possible structures in DMSO and aqueous solutions, respectively. TDDFT calculations indicated that the most possible forms in the studied media are locally excited at their λ_{\max} . However, the TDDFT calculations on the other neutral form in DMSO predicted that charge transfer is taken place through N=C=C-C moiety.

The developed method showed a wide calibration range for mesalazine. In addition, the method revealed high selectivity for mesalazine against some common ions, biologically active materials and pharmaceutical amines. MES was determined in different water matrices and pharmaceutical samples using the analytical method. The method is the first applicable sensing method for an amine in aqueous solutions based on a furan ring-opening reaction.

CRedit authorship contribution statement

Leila Sabahi-Agabager: Conceptualization, Methodology, Visualization, Investigation, Writing - original draft, Writing - review & editing. **Habibollah Eskandari:** Project administration, Supervision, Data curation, Validation, Writing - review & editing. **Farough Nasiri:** Project administration, Supervision, Writing - review & editing. **Amir Nasser Shamkhali:** Data curation, Methodology, Software, Writing - review & editing. **Somayyeh Baghi Sefidan:** Data curation, Methodology, Software, Writing - review & editing.

Declaration of Competing Interest

The authors declare that they have no known competing financial interests or personal relationships that could have appeared to influence the work reported in this paper.

Acknowledgements

The authors wish to acknowledge support of this work by the University of Mohaghegh Ardabili and the Iran National Science Foundation (INSF) [grant Number 96004838].

Appendix A. Supplementary material

Supplementary data to this article can be found online at <https://doi.org/10.1016/j.saa.2021.119846>.

References

- [1] R.F.A. Gomes, J.A.S. Coelho, C.A.M. Afonso, Synthesis and Applications of Stenhouse Salts and Derivatives, *Chem. Eur. J.* 24 (37) (2018) 9170–9186, <https://doi.org/10.1002/chem.201705851>.
- [2] O. Winkler, Beitrag zum Nachweis und zur Bestimmung von Oxymethylfurfural in Honig und Kunsthonig, *Z. Lebensm. Unters. Forsch.* 102 (3) (1955) 161–167, <https://doi.org/10.1007/BF01683776>.
- [3] K. CASTOLDI, M.I. MILANI, E.L. ROSSINI, L. PEZZA, H.R. PEZZA, Flow injection analysis of 5-(hydroxymethyl)-2-furaldehyde in honey by a modified Winkler method, *Anal. Sci.* 32 (4) (2016) 413–417, <https://doi.org/10.2116/analsci.32.413>.
- [4] M.I. Milani, E.L. Rossini, K. Castoldi, L. Pezza, H.R. Pezza, Paper platform for reflectometric determination of furfural and hydroxymethylfurfural in sugarcane liquor, *Microchem. J.* 133 (2017) 286–292, <https://doi.org/10.1016/j.microc.2017.03.046>.
- [5] P. Šafář, F. Považanec, N. Prónayová, P. Baran, G. Kicelbick, J. Kožíšek, M. Breza, Dichotomy in the Ring Opening Reaction of 5-[(2-Furyl) methylidene]-2, 2-dimethyl-1, 3-dioxane-4, 6-dione with Cyclic Secondary Amines, *Collect. Czech. Chem. Commun.* 65 (12) (2000) 1911–1938, <https://doi.org/10.1135/cccc20001911>.
- [6] S. Helmy, S. Oh, F.A. Leibfarth, C.J. Hawker, J. Read de Alaniz, Design and synthesis of donor–acceptor stenhouse adducts: a visible light photoswitch derived from furfural, *J. Org. Chem.* 79 (2014) 11316–11329, <https://doi.org/10.1021/jo502206g>.
- [7] S. Helmy, F.A. Leibfarth, S. Oh, J.E. Poelma, C.J. Hawker, J. Read de Alaniz, Photoswitching using visible light: a new class of organic photochromic molecules, *JACS* 136 (23) (2014) 8169–8172, <https://doi.org/10.1021/ja503016b>.
- [8] J.R. Hemmer, Z.A. Page, K.D. Clark, F. Stricker, N.D. Dolinski, C.J. Hawker, J. Read de Alaniz, Controlling Dark Equilibria and Enhancing Donor-Acceptor Stenhouse Adduct Photoswitching Properties through Carbon Acid Design, *JACS* 140 (33) (2018) 10425–10429, <https://doi.org/10.1021/jacs.8b06067>.
- [9] Y.J. Diaz, Z.A. Page, A.S. Knight, N.J. Treat, J.R. Hemmer, C.J. Hawker, J. Read de Alaniz, A versatile and highly selective colorimetric sensor for the detection of amines, *Chem. Eur. J.* 23 (15) (2017) 3562–3566, <https://doi.org/10.1002/chem.201700368>.
- [10] R. Saha, A. Devaraj, S. Bhattacharyya, S. Das, E. Zangrando, P.S. Mukherjee, Unusual Behavior of Donor-Acceptor Stenhouse Adducts in Confined Space of a Water-Soluble PdII8 Molecular Vessel, *JACS* 141 (21) (2019) 8638–8645, <https://doi.org/10.1021/jacs.9b03924>.
- [11] Y.-D. Cai, T.-Y. Chen, X.Q. Chen, X. Bao, Multiresponsive Donor-Acceptor Stenhouse Adduct: Opportunities Arise from a Diamine Donor, *Org. Lett.* 21 (18) (2019) 7445–7449, <https://doi.org/10.1021/acs.orglett.9b02753>.
- [12] S. Singh, P. Mai, J. Borowiec, Y. Zhang, Y. Lei, A. Schober, Donor–acceptor Stenhouse adduct-grafted polycarbonate surfaces: selectivity of the reaction for secondary amine on surface, *R. Soc. Open Sci.* 5 (7) (2018) 180207, <https://doi.org/10.1098/rsos.180207>.
- [13] A. Balamurugan, H.-i. Lee, A visible light responsive on–off polymeric photoswitch for the colorimetric detection of nerve agent mimics in solution and in the vapor phase, *Macromolecules* 49 (7) (2016) 2568–2574, <https://doi.org/10.1021/acs.macromol.6b00309>.
- [14] G. Noirbent, Y. Xu, A.-H. Bonardi, S. Duval, D. Gijmes, J. Lalevé, F. Dumur, New Donor-Acceptor Stenhouse Adducts as Visible and Near Infrared Light Polymerization Photoinitiators, *Molecules* 25 (2020) 2317, <https://doi.org/10.3390/molecules25102317>.
- [15] Q. Yan, C. Li, S. Wang, Z. Lin, Q. Yan, D. Cao, Visible light responsive donor-acceptor stenhouse adducts with indoline-tri/tetra-phenylethylene chromophore: synthesis, aggregation-induced emission, photochromism and solvent dependence effect, *Dyes Pigm.* 178 (2020) 108352, <https://doi.org/10.1016/j.dyepig.2020.108352>.
- [16] Q. Chen, Y.J. Diaz, M.C. Hawker, M.R. Martinez, Z.A. Page, S. Xiao-An Zhang, C.J. Hawker, J. Read de Alaniz, Stable Activated Furan and Donor-Acceptor Stenhouse Adduct Polymer Conjugates as Chemical and Thermal Sensors, *Macromolecules* 52 (11) (2019) 4370–4375, <https://doi.org/10.1021/acs.macromol.9b00533>.
- [17] N. Shahabadi, S.M. Fili, Molecular modeling and multispectroscopic studies of the interaction of mesalamine with bovine serum albumin, *Spectrochim. Acta A Mol. Biomol. Spectrosc.* 118 (2014) 422–429, <https://doi.org/10.1016/j.saa.2013.08.110>.
- [18] A. Pandith, G. Hazra, H.-S. Kim, A new fluorogenic sensing platform for salicylic acid derivatives based on π - π and NH- π interactions between electron-deficient and electron-rich aromatics, *Spectrochim. Acta A Mol. Biomol. Spectrosc.* 178 (2017) 151–159, <https://doi.org/10.1016/j.saa.2017.01.053>.
- [19] E. Pastorini, M. Locatelli, P. Simoni, G. Roda, E. Roda, A. Roda, Development and validation of a HPLC-ESI-MS/MS method for the determination of 5-aminosalicylic acid and its major metabolite N-acetyl-5-aminosalicylic acid in human plasma, *J. Chromatogr. B* 872 (1–2) (2008) 99–106, <https://doi.org/10.1016/j.jchromb.2008.07.026>.
- [20] M. Nobilis, Z. Vybíralová, K. Sládková, M. Lísa, M. Holčápek, J. Květina, High-performance liquid-chromatographic determination of 5-aminosalicylic acid and its metabolites in blood plasma, *J. Chromatogr. A* 1119 (1–2) (2006) 299–308, <https://doi.org/10.1016/j.chroma.2006.01.058>.
- [21] J.A. Rafael, J.R. Jabor, R. Casagrande, S.R. Georgetti, M.d.F. Borin, M.J.V. Fonseca, Validation of HPLC, DPPH• and nitrosation methods for mesalamine determination in pharmaceutical dosage forms, *Rev. de Cienc. Farm. Básica e Apl.* 43 (1) (2007) 97–103, <https://doi.org/10.1590/S1516-93322007000100012>.
- [22] A.B. Teradale, S.D. Lamani, P.S. Ganesh, B.E.K. Swamy, S.N. Das, CTAB immobilized carbon paste electrode for the determination of mesalazine: A cyclic voltammetric method, *Sens. Biosensing Res.* 15 (2017) 53–59, <https://doi.org/10.1016/j.sbsr.2017.08.001>.
- [23] M. Štěpánková, R. Šelešovská, L. Janíková, J. Chýlková, Voltammetric determination of mesalazine in pharmaceutical preparations and biological samples using boron-doped diamond electrode, *Chem PAP* 71 (8) (2017) 1419–1427, <https://doi.org/10.1007/s11696-017-0135-6>.
- [24] A. Akkaya, C. Altug, N. Pazarlioglu, E. Dinckaya, Determination of 5-Aminosalicylic Acid by Catalase-Peroxidase Based Biosensor, *Electroanalysis* (N.Y.N.Y.) 21 (16) (2009) 1805–1810, <https://doi.org/10.1002/elan.200904606>.
- [25] N. Nataraj, S.K. Krishnan, T.-W. Chen, S.-M. Chen, B.-S. Lou, Ni-Doped ZrO 2 nanoparticles decorated MW-CNT nanocomposite for the highly sensitive electrochemical detection of 5-amino salicylic acid, *Analyst* 146 (2) (2021) 664–673, <https://doi.org/10.1039/D0AN01507E>.
- [26] S. Ebrahimi, A. Afkhami, T. Madrakian, Enhanced electrochemical responses at supramolecularly modified graphene: Simultaneous determination of sulphasalazine and its metabolite 5-aminosalicylic acid, *J. Electroanal. Chem.* 838 (2019) 186–194, <https://doi.org/10.1016/j.jelechem.2019.03.001>.
- [27] T.S. Kanna Sharma, K.-Y. Hwa, A. Santhan, A. Ganguly, Synthesis of novel three-dimensional flower-like cerium vanadate anchored on graphitic carbon nitride as an efficient electrocatalyst for real-time monitoring of mesalazine in biological and water samples, *Sens. Actuators B Chem.* 331 (2021) 129413, <https://doi.org/10.1016/j.snb.2020.129413>.
- [28] J. Vinoth Kumar, T. Kokulnathan, S.-M. Chen, T.-W. Chen, A.M. Elgorban, M.S. Elshikh, N. Marraiki, E.R. Nagarajan, Two-dimensional copper tungstate nanosheets: application toward the electrochemical detection of mesalazine, *ACS Sustain. Chem. Eng.* 7 (22) (2019) 18279–18287, <https://doi.org/10.1021/acssuschemeng.9b02171>.
- [29] B. Nigović, A. Mornar, E. Brusač, M.-L. Jeličić, Selective sensor for simultaneous determination of mesalazine and folic acid using chitosan coated carbon nanotubes functionalized with amino groups, *J. Electroanal. Chem.* 851 (2019) 113450, <https://doi.org/10.1016/j.jelechem.2019.113450>.
- [30] R. Gotti, R. Pomponio, C. Bertucci, V. Cavrini, Determination of 5-aminosalicylic acid related impurities by micellar electrokinetic chromatography with an ion-pair reagent, *J. Chromatogr. A* 916 (1–2) (2001) 175–183, [https://doi.org/10.1016/S0021-9673\(00\)01097-9](https://doi.org/10.1016/S0021-9673(00)01097-9).
- [31] K. Maráková, J. Piešťanský, P. Mikuš, Determination of drugs for Crohn's disease treatment in pharmaceuticals by capillary electrophoresis hyphenated with tandem mass spectrometry, *Chromatographia* 80 (4) (2017) 537–546, <https://doi.org/10.1007/s10337-016-3213-y>.
- [32] E.J. Llorent-Martínez, P. Ortega-Barrales, M.L. Fernández de Córdova, A. Ruiz-Medina, Development of an automated chemiluminescence flow-through sensor for the determination of 5-aminosalicylic acid in pharmaceuticals: a comparative study between sequential and multicommutated flow techniques, *Anal. Bioanal. Chem.* 394 (3) (2009) 845–853, <https://doi.org/10.1007/s00216-009-2757-1>.
- [33] A.A. Elbashir, F. Altayib Alasha Abdalla, H.Y. Aboul-Enein, Host-guest inclusion complex of mesalazine and β -cyclodextrin and spectrofluorometric determination of mesalazine, *Luminescence* 30 (4) (2015) 444–450, <https://doi.org/10.1002/bio.v30.410.1002/bio.2758>.
- [34] A.A. Elbashir, F.A.A. Abdalla, H.Y. Aboul-Enein, Supramolecular interaction of 18-crown-6 ether with mesalazine and spectrofluorimetric determination of mesalazine in pharmaceutical formulations, *Luminescence* 30 (8) (2015) 1250–1256, <https://doi.org/10.1002/bio.2888>.
- [35] F.-L. Cui, L.-X. Qin, F. Li, H.-X. Luo, Synchronous fluorescence determination and molecular modeling of 5-Aminosalicylic acid (5-ASA) interacted with human serum albumin, *J. Mol. Model.* 14 (12) (2008) 1111–1117, <https://doi.org/10.1007/s00894-008-0352-6>.
- [36] B.S. Chandra, S.S. Bhogela, M. Shaik, C.S. Vadlamudi, M. Chappa, N.S. Maddirala, Simple and sensitive spectrophotometric methods for the analysis of mesalazine in bulk and tablet dosage forms, *Quim. Nova* 34 (2011) 1068–1073, <https://doi.org/10.1590/S0100-40422011000600026>.
- [37] F. Alasha Abdalla, A. Elbashir, Development and Validation of spectrophotometric methods for the determination of mesalazine in pharmaceutical formulation, *Med. Chem.* 4 (2014) 361–366, <https://doi.org/10.4172/2161-0444.1000166>.
- [38] S.B. Sefidan, H. Eskandari, A.N. Shamkhali, Rapid colorimetric flow injection sensing of hypochlorite by functionalized graphene quantum dots, *Sens. Actuators B Chem.* 275 (2018) 339–349, <https://doi.org/10.1016/j.snb.2018.08.023>.
- [39] S.B. Sefidan, H. Eskandari, Sensitive assay of pharmaceutical amines in environmental samples and formulations by oxygenated graphene quantum dots, *Measurement* 132 (2019) 292–302, <https://doi.org/10.1016/j.measurement.2018.09.063>.
- [40] S.Y. Garmonov, Z.C. Nguyen, I.F. Mingazetdinov, L.M. Yusupova, N.S. Shitova, R. N. Ismailova, V.F. Sopin, Spectrophotometric determination of mesalazine in urine for assessing the acetylation phenotype in vivo in humans, *Pharm. Chem. J.* 45 (12) (2012) 757–760, <https://doi.org/10.1007/s11094-012-0719-y>.
- [41] N.J. Thumar, M.P. Patel, Synthesis, characterization, and antimicrobial evaluation of carbostyryl derivatives of 1H-pyrazole, *Saudi Pharm. J.* 19 (2) (2011) 75–83, <https://doi.org/10.1016/j.jpsp.2011.01.005>.

- [42] J.R. Hemmer, S.O. Poelma, N. Treat, Z.A. Page, N.D. Dolinski, Y.J. Diaz, W. Tomlinson, K.D. Clark, J.P. Hooper, C. Hawker, J. Read de Alaniz, Tunable visible and near infrared photoswitches, *JACS* 138 (42) (2016) 13960–13966, <https://doi.org/10.1021/jacs.6b07434>.
- [43] F. Jensen, *Introduction to computational chemistry, second ed.*, John Wiley & sons, West Sussex, 2007.
- [44] C.A. Ullrich, *Time-dependent density-functional theory: concepts and applications*, OUP Oxford, New York, 2011.
- [45] A. Pałasz, A Green Approach to the Synthesis of Fused Uracils: Pyrano [2, 3-d] pyrimidines: 'On-Water' One-Pot Synthesis by Domino Knoevenagel/Diels-Alder Reactions, *Synthesis* 2010 (2010) 4021–4032, <https://doi.org/10.1055/s-0030-1258292>.
- [46] M.L. Deb, P.J. Bhuyan, Uncatalysed Knoevenagel condensation in aqueous medium at room temperature, *Tetrahedron Lett.* 46 (38) (2005) 6453–6456, <https://doi.org/10.1016/j.tetlet.2005.07.111>.
- [47] C. Verrier, S. Moebs-Sanchez, Y. Queneau, F. Popowycz, The Piancatelli reaction and its variants: recent applications to high added-value chemicals and biomass valorization, *Org. Biomol. Chem.* 16 (5) (2018) 676–687, <https://doi.org/10.1039/C7OB02962D>.
- [48] O. Nieto Faza, C. Silva Lopez, R. Álvarez, Á.R. de, Lera, Theoretical study of the electrocyclic ring closure of hydroxypentadienyl cations, *Chem. Eur. J.* 10 (2004) 4324–4333, <https://doi.org/10.1002/chem.200400037>.
- [49] N. Mallo, A. Tron, J. Andréasson, J.B. Harper, L.S. Jacob, N.D. McClenaghan, G. Jonusauskas, J.E. Beves, Hydrogen-bonding donor-acceptor Stenhouse adducts, *ChemPhotoChem* (2020), <https://doi.org/10.1002/cptc.201900295>.
- [50] N. Mallo, P.T. Brown, H. Iranmanesh, T.S.C. MacDonald, M.J. Teusner, J.B. Harper, G.E. Ball, J.E. Beves, Photochromic switching behaviour of donor-acceptor Stenhouse adducts in organic solvents, *ChemComm.* 52 (93) (2016) 13576–13579, <https://doi.org/10.1039/C6CC08079K>.
- [51] J.-D. Chai, M. Head-Gordon, Systematic optimization of long-range corrected hybrid density functionals, *J. Chem. Phys.* 128 (8) (2008) 084106, <https://doi.org/10.1063/1.2834918>.
- [52] H. Iikura, T. Tsuneda, T. Yanai, K. Hirao, A long-range correction scheme for generalized-gradient-approximation exchange functionals, *J. Chem. Phys.* 115 (8) (2001) 3540–3544, <https://doi.org/10.1063/1.1383587>.
- [53] M.M. Francl, W.J. Pietro, W.J. Hehre, J.S. Binkley, M.S. Gordon, D.J. DeFrees, J.A. Pople, Self-consistent molecular orbital methods. XXIII. A polarization-type basis set for second-row elements, *J. Chem. Phys.* 77 (7) (1982) 3654–3665, <https://doi.org/10.1063/1.444267>.
- [54] M.W. Schmidt, K.K. Baldridge, J.A. Boatz, S.T. Elbert, M.S. Gordon, J.H. Jensen, S. Koseki, N. Matsunaga, K.A. Nguyen, S. Su, T.L. Windus, M. Dupuis, J.A. Montgomery, General atomic and molecular electronic structure system, *J. Comput. Chem.* 14 (11) (1993) 1347–1363, <https://doi.org/10.1002/jcc.540141112>.
- [55] B. Mennucci, R. Cammi, J. Tomasi, Excited states and solvatochromic shifts within a nonequilibrium solvation approach: A new formulation of the integral equation formalism method at the self-consistent field, configuration interaction, and multiconfiguration self-consistent field level, *J. Chem. Phys.* 109 (7) (1998) 2798–2807, <https://doi.org/10.1063/1.476878>.
- [56] A.V. Marenich, C.J. Cramer, D.G. Truhlar, Universal solvation model based on solute electron density and on a continuum model of the solvent defined by the bulk dielectric constant and atomic surface tensions, *J. Phys. Chem. B.* 113 (18) (2009) 6378–6396, <https://doi.org/10.1021/jp810292n>.
- [57] F. Furche, R. Ahlrichs, Adiabatic time-dependent density functional methods for excited state properties, *J. Chem. Phys.* 117 (16) (2002) 7433–7447, <https://doi.org/10.1063/1.1508368>.
- [58] T. Lu, F. Chen, Multiwfn: a multifunctional wavefunction analyzer, *J. Comput. Chem.* 33 (5) (2012) 580–592, <https://doi.org/10.1002/jcc.22885>.
- [59] D.L. French, J.W. Mauger, Evaluation of the physicochemical properties and dissolution characteristics of mesalamine: relevance to controlled intestinal drug delivery, *Pharm. Res.* 10 (1993) 1285–1290, <https://doi.org/10.1023/A:1018909527659>.
- [60] K. Box, C. Bevan, J. Comer, A. Hill, R. Allen, D. Reynolds, High-throughput measurement of p K a values in a mixed-buffer linear pH gradient system, *Anal. Chem.* 75 (4) (2003) 883–892, <https://doi.org/10.1021/ac020329y>.
- [61] I.M. Kolthoff, M.K. Chantooni, Substituent effects on dissociation of benzoic acids and heteroconjugation of benzoates with p-bromophenol in acetonitrile, N, N-dimethylformamide, and dimethyl sulfoxide. Intramolecular hydrogen bonding in o-hydroxybenzoic acids and their anions, *JACS.* 93 (16) (1971) 3843–3849, <https://doi.org/10.1021/ja00745a001>.
- [62] P.J. Taylor, G. van der Zwan, L. Antonov, *Tautomerism: Introduction, history, and recent developments in experimental and theoretical methods*, in: L. Antonov (Ed.), *Tautomerism: methods and theories*, Wiley-VCH Verlag GmbH & Co. KGaA, Weinheim, 2014, pp. 1–24.
- [63] A.D. Dubonosov, V.A. Bren, V.I. Minkin, Enolimine-Ketoenamine Tautomerism for Chemosensing, in: L. Antonov (Ed.), *Tautomerism: Concepts and Applications in Science and Technology*, Wiley-VCH Verlag GmbH & Co. KGaA, Weinheim, 2016, pp. 229–251.
- [64] D.A. Skoog, D.M. West, F.J. Holler, S.R. Crouch, *Fundamentals of Analytical Chemistry*, ninth ed., Cengage Learning, Belmont, 2013.
- [65] D.C. Montgomery, *Design and analysis of experiments*, ninth ed., John Wiley & sons, Hoboken, 2017.
- [66] H. Hadi, Continuous flow injection spectrophotometric determination of mesalazine in pharmaceutical forms, *Syst. Rev. Pharm.* 12 (2021) 202–208, <https://doi.org/10.31838/srp.2021.2.25>.
- [67] Y. Hu, Y. Wang, R. Guan, C. Zhang, X. Shao, Q. Yue, Construction of a ratio fluorescence assay of 5-aminosalicylic acid based on its aggregation induced emission with blue emitting N/P-codoped carbon dots, *RSC Adv.* 11 (12) (2021) 6607–6613, <https://doi.org/10.1039/D0RA10258J>.